Effect of unusually elevated SO_2 atmospheric content on the corrosion of high power electrical conductors – Part 3. Pure copper

Rosa Vera [a], Diana Delgado [a], Blanca M. Rosales [b,1,*]

[a] Corrosion Laboratory, Institute of Chemistry, Pontificia Universidad Católica de Valparaíso, Chile
[b] CIDEPINT, Av. 52 s/n, entre 121 y 122, B1900AYB, La Plata, Argentina

Abstract

This research work belongs to a series of studies simultaneously performed with two previous publications in this journal as Part I. Al and 6201 Al alloy and Part 2. Pure copper. The aim of the project was to have a comparative picture of the joint effect of marine and industrial atmospheric pollutants on the corrosion resistance of wire metals employed for high power electric transmission. This one is also based on the pure Cu behaviour, but limited to six marine-industrial atmospheres with extremely high SO_2 contents. The interest in this study was triggered by unusual results considered appropriate to investigate. Weight loss after 4 and 11 months exposure was determined and morphology of the attack was analysed through SEM–ESEM–EDX. Polarisation of samples after exposure to all the test sites as compared to bare Cu clarified the effect of unusually high SO_2 pollutant contents in these atmospheres on the high protectiveness of the corrosion products formed.
© 2007 Published by Elsevier Ltd.

1. Introduction

The main purpose of copper application is based on its well known ability to develop protective and attractive corrosion products designed patina. Its traditional use as architectural material had not been previously explored in aggressive atmospheres such as in the present study. The comparative susceptibility to atmospheric corrosion was focused in the interest of making an important material selection for electricity transmission infrastructure in the Fifth Chilean Region. This metal is also used for electric conductors due to its high conductivity, important property in communication and electronic industries.

Studies on the atmospheric corrosion of copper and its alloys have been performed through natural outdoor exposure [1–7], as in laboratory [8] and in both [9]. However, there were not previous studies in as high SO_2 concentrations as those measured in this work.

The colours of the corrosion products formed during outdoor exposure vary from pink-salmon to dark brown finally adopting a green shade, the main traditional characteristic attributed to patina corrosion products.

According to a previous paper the first definition of copper patina in corrosion terms was conceived as a barrier product film with a minimum set of protectiveness properties promoting the long term structural integrity of the base metal [10].

For a gas attack on a surface it is essential its dissolution in the aqueous phase deposited on the metal. For low concentrations and slow reaction with the metal there will be a gas equilibrium distribution between the vapor and liquid phases given by Henry's law, according to which the gas concentration in the liquid is proportional to its partial

* Corresponding author. Tel./fax: +54 11 4782 9921.
  E-mail addresses: rvera@ucv.cl (R. Vera), brosales@fibertel.com.ar (B.M. Rosales).
1 Researcher of the Consejo Nacional de Investigaciones Científicas y Técnicas (CONICET).

pressure in the gas phase. Once reached the wet metal surface SO_2 is oxidized to SO_4H_2 due to the presence of atmospheric O_2 [11]. The high acid solubility in water produces its dissociation and successive attack to the metal surface. For the very high SO_2 atmospheric partial pressure it is probable to be far from an equilibrium situation according to Henry's law.

The metal corrosion rate is thus under mixed control by the delivery rate of the aggressive constituents and of their surface reaction rate. In the present case the probable controlling rate will be the metal surface attack while the transport rate of aggressive agents would be negligible due to the elevated SO_2 concentrations. The airflow velocity on the copper atmospheric corrosion rate was studied in a laboratory exposure with controlled aerodynamic conditions by Volpe et al. [12]. The corrosion rate increased almost linearly with airflow velocity up to 0.2 m/s suggesting that the limited rate was the transport of corrosive matter to the surface. Above that velocity the corrosion rate decreased in this particular example suggesting that surface reactions were the rate-limiting factor.

Amongst the knowledge development achieved by the multinational Atmospheric Corrosion studies (MICAT, ISOCORRAG and UN/ECE) the many data base collected with the same methodology in real atmospheres covering a great part of the World these cooperative projects allowed to develop a very useful new tool. The Dose Response Functions, which application is interesting not only from the scientific point of view but also to provide quick corrosion estimation in Regions which corrosiveness was not already determined [13].

As well as in the two previous studies of this project [14,3] various relevant differences as compared to most atmospheric corrosion publications are in the tested materials and in the exposure test sites were involved. Copper was exposed as wires instead of as flat samples, having thus determined increased corrosion rates [14,3,15,16]. These atmospheres contain very high industrial SO_2 pollutant contents and various Cl^- levels associated to marine atmospheres combined in different proportions in natural environments. Soil dry deposition in these sites is higher than the expected for ground finishing according to the ISO standard 9223 [17]. The total test duration was shorter than in the two previous works, but long enough to provide information on the patina growth mechanism in SO_2 heavily polluted sites.

As it is well known, patina on copper is the result of the chemical interaction of trace contaminants in the atmosphere, mainly SO_2 and chlorides. But nothing was already discussed about very high SO_2 pollutant contents. Its composition and morphology depend on the geographic localisation of the test site, climatic conditions and contaminant deposition rates [1–6]. In that context, one of the main interests in this study was to determine the top limit in the atmospheric SO_2 content to form patinas. May the accumulated corrosion products on Cu samples in these extremely high SO_2 polluted test sites, be considered "patinas"?

In corrosion terms as protectiveness, measured through the slope of the corrosion rate as a function of time or by polarisation after different exposition times, in fact we demonstrated that they are.

2. Experimental

In the previous studies, 17 marine and marine-industrial sites were selected. This study is limited to the 6 marine-industrial sites where the highest SO_2 concentrations were observed. Test stations are at distances ranging from 600 m to 2000 m to the sea, between 400 m and 1200 m from an industrial plant, the only SO_2 pollutant source, and at slightly different altitudes from 11 to 47 m over the sea level (osl).

Tests samples were 99.0% Cu, as received stranded wires of 2.50 mm diameter, cut to 1000 mm length. The specimens were formed as open helixes around a 24 mm diameter mandrill. Crevice by contact with other material or with adjacent spires was avoided. Two replicates were exposed at the outdoor atmospheres, fixed by their isolated ends at 45° angle to the horizon, during 4 and 11 months.

The methodology for the atmospheric characterisation and weight loss determinations followed ISO 9223 to 9226 [17–20] and ISO 8407 [21] standards, respectively.

Morphology in plan and in polished transversal cross section after the tested samples expositions were analysed through scanning electron microscopy using a SEM Philips 515 coupled to an EDAX 9100 analyser for elemental characterisation. Also an environmental ESEM–EDAX Philips XL 30 was applied to polished cross sections for the mechanism analysis of the corrosion attack nucleation and propagation.

X-ray diffraction analysis was applied to the corrosion products formed at each test site after both exposure periods. A SIEMENS D 5000 with $CuK\alpha$ radiation and a graphite monochromator 40 KV/30 mA, in the scanning range 05–70°, were used.

Electrochemical polarisation was applied to weathered copper samples from all the test sites as compared to non-exposed bare Cu as witness. The anodic curves were obtained in 0.1 M Na_2SO_4 electrolyte after solution deaeration by 99.99% N_2 bubbling and cathodic ones in air saturated solutions, at 100 mV min^{-1} potential scan rate, with constant magnetic stirring to maintain constant the hydrodynamics of the electrolyte. A conventional Pyrex glass cell with a Pt counter electrode and a saturated calomel electrode as reference, through a Luggin capillary, were used.

3. Results

The test sites location data, pollutant deposition rates, classification of the atmospheres according to ISO 9224 standard [18] and corrosion product colours after exposure are displayed in Table 1. Data for the colour comparison respect to products formed at marine test stations 2 and 27 of a previous paper [3], are for site 27 grayish products,

Table 1
Location and ambient characteristics of the 6 marine-industrial test sites at Ventana, Chile

Station (No.)	Sea dist. (m)	Cl⁻ ($mg\,m^{-2}\,day^{-1}$)	Height osl (m)	Distance to SO_2 source (m)	SO_2 ($mg\,m^{-2}\,day^{-1}$)	ISO Cat.[a]	Patina colour 4–11 months
10	760	32.0	30	1200	86.8	P_3	Reddish, black points, greenish
14	1220	28.3	41	1200	94.4	P_3	Reddish, greenish[b]
4	1980	18.6	47	1200	103.8	P_3	Greenish[b]
13	600	17.5	13	400	240.4	$>P_3$	Greenish
9	660	21.3	12	400	282.3	$>P_3$	Greenish
5	690	20.4	11	400	651.2	$>P_3$	Greenish

[a] Pollutants (P) and salinity (S) ISO categories. All sites are (S_1), according to ISO 9224 standard [18].
[b] The green products are not uniformly distributed.

very few green not uniformly distributed and for site 2 the same as 27 but more intense green shade than products formed in these sites.

The yearly meteorological parameters of the region involving the test sites, temperature (*T*), relative humidity (RH), predominant winds and rains and time of wetness (TOW) during a 4 year period involving this study are shown in Fig. 1a–d as a function of time. The traverse board of the same area, shown in Fig. 2 of both previous papers [14,3], evidenced that SW yearly predominant winds were the salt fog supplier to the test stations. Depending on the distance to the sea shore line, the relative height osl of

the test sites and the more or less screen action of obstacles diverse amount of fog reached the different test sites.

Also a croquis of the Fifth Region seashore zone of Valparaiso, Chile (Lat. 32°S, Long. 71°W) where the 6 marine-industrial test sites were installed, can be seen in a recent publication in this periodical [3]. The samples exposure was performed at the beginning of summer.

The main components of the corrosion products determined through X-ray diffraction are shown in Table 2, after both periods in each atmosphere.

Fig. 2 depicts the copper mass loss as a function of time at all the test sites in the 6 marine-industrial environments.
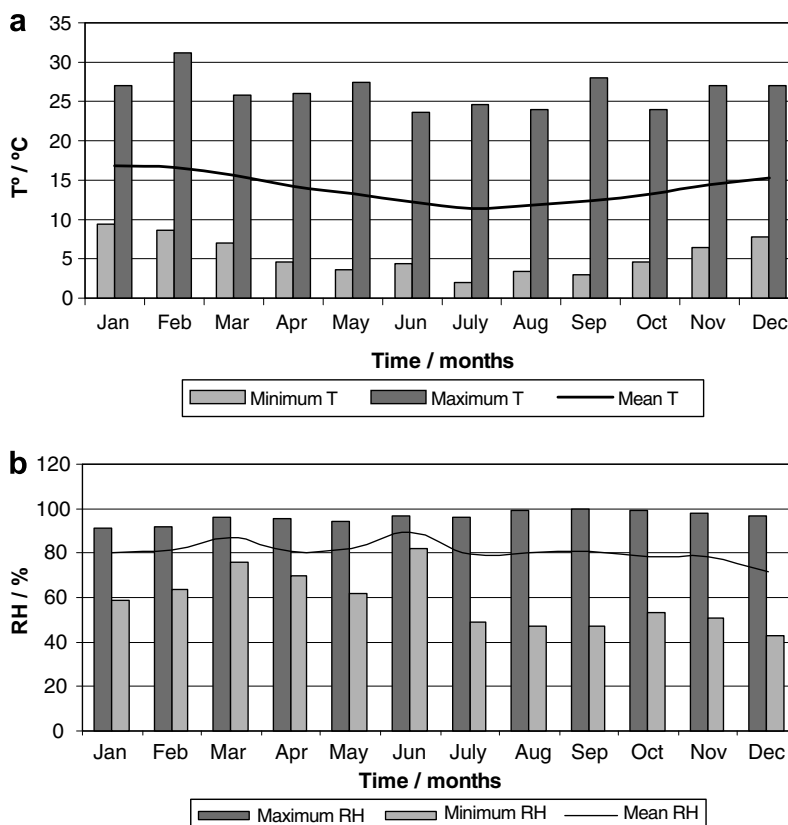

Fig. 1. Meteorological parameters in the Fifth Region, Chile, with time (period 1970–2003). (a) Extreme and mean temperature. (b) Extreme and mean relative humidity. (c) Mean rainfall and maximum wind speed. (d) Time of wetness during the period June 2002–August 2005.
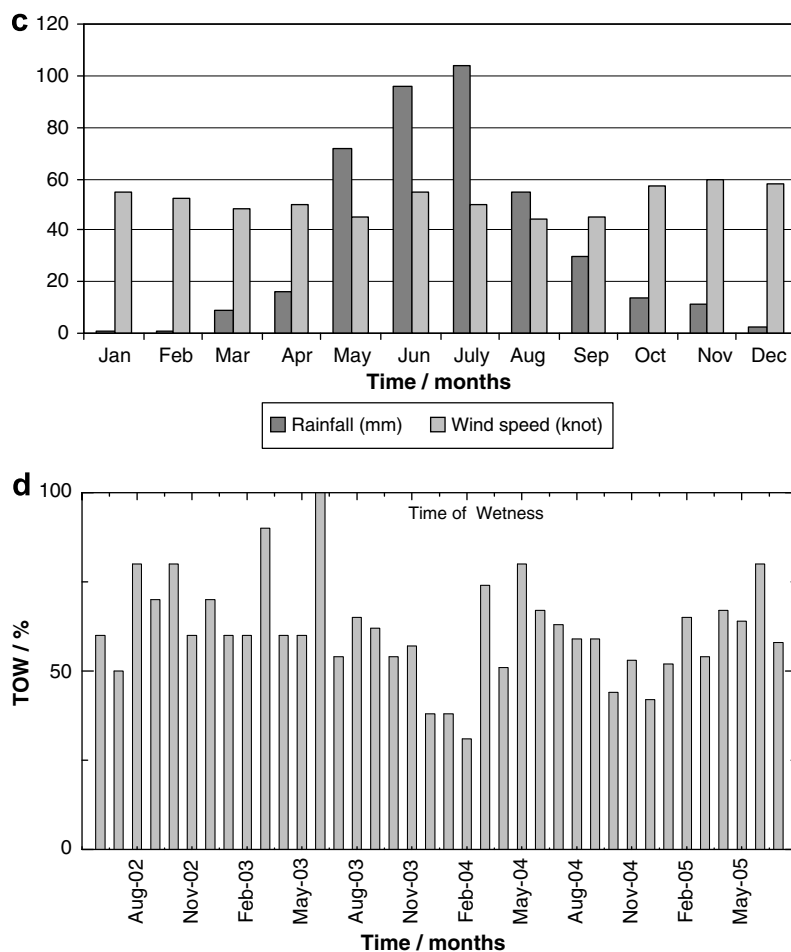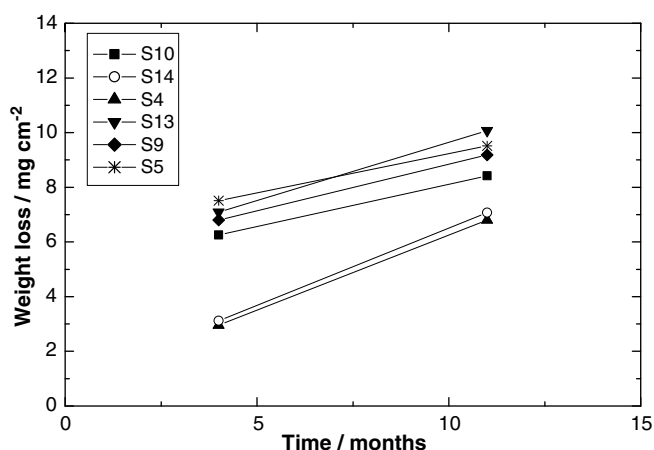
Fig. 1 (*continued*)

Fig. 2. Weight loss of copper in the 6 marine-industrial stations in function of the exposure time.

Fig. 3 shows plan morphologies and EDX on the copper corrosion products in all sites after 4 and 11 months exposure.

Fig. 4a shows the polished transverse cross section of samples exposed for 4 and 11 months at sites 10,14, 4, 13 and 9; b shows detailed ESEM–EDX at different magnifi-

cations of site 5, after 11 months exposure and c shows a longitudinal cross section after 4 months exposure at site 4.

In Fig. 5a and b a comparison is shown of pickled samples in the most highly SO_2 polluted site 5 with the typical intergranular attack of the most highly contaminated in Cl^- from site 2 after 11 months.

In Fig. 6 anodic and cathodic polarisation of copper after 4 and 11 months exposure in all the test sites are shown as compared to non-exposed bare copper. The protectiveness increase with the SO_2 atmospheric content was one of the unexpected behaviours suggesting this detailed study.

Fig. 7a and b displays the polarisation of copper in 0.1 M Na_2SO_4 solution after exposition in the marine-industrial site 5 with the highest SO_2. The latter results in this environment were the main for a deeper analysis of the copper behaviour not found when the 17 sites were investigated. The structural ESEM aspect modifications shown in Fig. 7c, at the 3 plateaux potentials during anodic polarisation are also reflected in the EDX results of the corrosion products, as can be seen in Fig. 7d.

Fig. 8, the slope of graphs in Fig. 2 as a function of copper exposure time in all the atmospheres after 4 and 11 months exposure evidenced the protectiveness variation

Table 2
X-ray diffraction of the corrosion products formed on copper in the 6 marine-industrial test sites after the two exposure periods

Station	4 Months	11 Months
S10	Carbon (M)	Carbon (M)
	Cuprite (Cu_2O) (M)	Cuprite (Cu_2O) (M)
	Tenorite (CuO) (m)	Tenorite (CuO) (m)
	Atacamite ($Cu_2Cl(OH)_3$) (m)	Quartz (SiO_2) (m)
		Atacamite ($Cu_2Cl(OH)_3$) (m)
S14	Cuprite (Cu_2O) (M)	Cuprite (Cu_2O) (M)
	Sodium chloride (NaCl) (M)	Tenorite (CuO) (t)
		Sodium chloride (NaCl) (M)
		Quartz (SiO_2) (m)
		Posnjankite ($CuSO_4 \cdot 3Cu(OH)_2 \cdot 2H_2O$) (m)
S4	Cuprite (Cu_2O) (M)	Cuprite (Cu_2O) (M)
	Chalcocite (Cu_2S) (m)	Sodium Chloride (NaCl) (M)
	Sodium chloride (NaCl) (M)	Posnjankite ($CuSO_4 \cdot 3Cu(OH)_2 \cdot 2H_2O$) (m)
S13	Cuprite (Cu_2O) (M)	Cuprite (Cu_2O) (M)
	Sodium chloride (NaCl) (M)	Posnjankite ($CuSO_4 \cdot 3Cu(OH)_2 \cdot 2H_2O$) (m)
	Posnjankite ($CuSO_4 \cdot 3Cu(OH)_2 \cdot 2H_2O$) (M)	Brochantite ($CuSO_4 \cdot 3Cu(OH)_2$) (m)
S9	Quartz (SiO_2) (m)	Cuprite (Cu_2O) (m)
	Cuprite (Cu_2O) (m)	Quartz (SiO_2) (m)
	Calcium carbonate ($CaCO_3$) (m)	($CuSO_4 \cdot 3Cu(OH)_2 \cdot 2H_2O$) (m)
	Posnjankite ($CuSO_4 \cdot 3Cu(OH)_2 \cdot 2H_2O$) (M)	Brochantite ($CuSO_4 \cdot 3Cu(OH)_2$) (m)
S5	Chalcopyrite ($CuFeS_2$) (t)	Chalcopyrite ($CuFeS_2$) (t)
	Cuprite (Cu_2O) (m)	Cuprite (Cu_2O) (m)
	Sodium chloride (NaCl) (M)	Tenorite (CuO) (t)
	Posnjankite ($CuSO_4 \cdot 3Cu(OH)_2 \cdot 2H_2O$) (M)	Chalcocite (Cu_2S) (m)
		Copper sulphate (Cu_2SO_4) (M)
		Sodium Chloride (NaCl) (M)
		Posnjankite ($CuSO_4 \cdot 3Cu(OH)_2 \cdot 2H_2O$) (m)
		Brochantite ($CuSO_4 \cdot 3Cu(OH)_2$) (m)

M = major, m = minor and t = traces.

amongst the sites through their relative values and slopes. Most protective product films were found at site 5, coincident with the greatest variety of copper corrosion products, highest SO_2 in the atmosphere as well as S through EDX, after site 9 for the first period and the main after the second one.

The comparative morphologies in plan as well as in cross section in Figs. 3 and 4 show greater particle sizes after 4 than after 11 months exposure. These can be associated to a faster nucleation on less covered surfaces than after the corrosion products film growth decreased the pollutants effect. The particle size decrease with time must also

be caused by successive re-crystallisation during dissolution precipitation processes. The compactness increase with time revealed in the cross section morphology also explains the corrosion products protectiveness increase with exposure.

Fig. 9 summarises the weight loss of copper in the 6 marine-industrial stations for both exposure times as a function of the very similar (a) SO_2 and (b) total pollutant content of the test sites.

Fig. 10 shows the maximum and minimum weight loss deviation of copper weight loss in marine-industrial stations 4 and 13, respectively.

4. Discussion

According to ISO 9225 standard [19] the maximum pollutant SO_2 considered for category classification is 200 mg m^{-2} d^{-1} and designed P3. It can be seen from Table 1 that this limit is surpassed in the 3 last marine-industrial test sites designed as 13, 9 and 5 by factors 1.2, 1.4 and 3.3. Thus, very high corrosion rates could have been expected for the copper samples exposed at these test sites, as were measured for Al and its 6201 alloy [14].

4.1. Weight loss analyses

Good correlation between mass loss and exposure time was always found, as can be seen in Fig. 2, even when not in the relative order according to the atmospheric pollutants contents. In fact, the 2 lowest parallel lines corresponding to site 4 and then site 14, do not correspond to the lowest SO_2 pollutant levels. However, their relative weight losses seem mainly to be related to their distance to the sea shore, and even the low proportion of Cl^- seems to be the controlling pollutant, for almost similar SO_2.

Also all the slopes set did not produce the expected results respect to the atmospheric Cl^- and SO_2 effects with time. In fact, for similar low chloride contents the measured weight losses were not always proportional to the diverse SO_2 concentration. The most sticking lack of correlation the SO_2 pollutant content was found between sites 9 and 5, for almost the same Cl^-, but 2.3 SO_2. Increasing weight losses for both exposure periods produced around 10% corrosion rate levels increase for more than twice SO_2 concentration. Also in Fig. 2 the very near lines found for sites 9 and 10, for small difference in Cl^-, does not seem to be proportionally affected by the higher 3.2 times SO_2 deposition rate at site 9 than to 10.

According to these results another more important factor must control the weight loss in these test sites, being the distance to the sea line. However, the fog arrived to the samples did not proportionally affect the Cl^- but certainly decide the TOW determining the "real" SO_2 pollutant available as electrolyte for corrosion. It is the amount of dissolved in the water included on the corrosion product samples which effectively participates. Thus, the corrosiveness of a site would not be proportional to the environmental
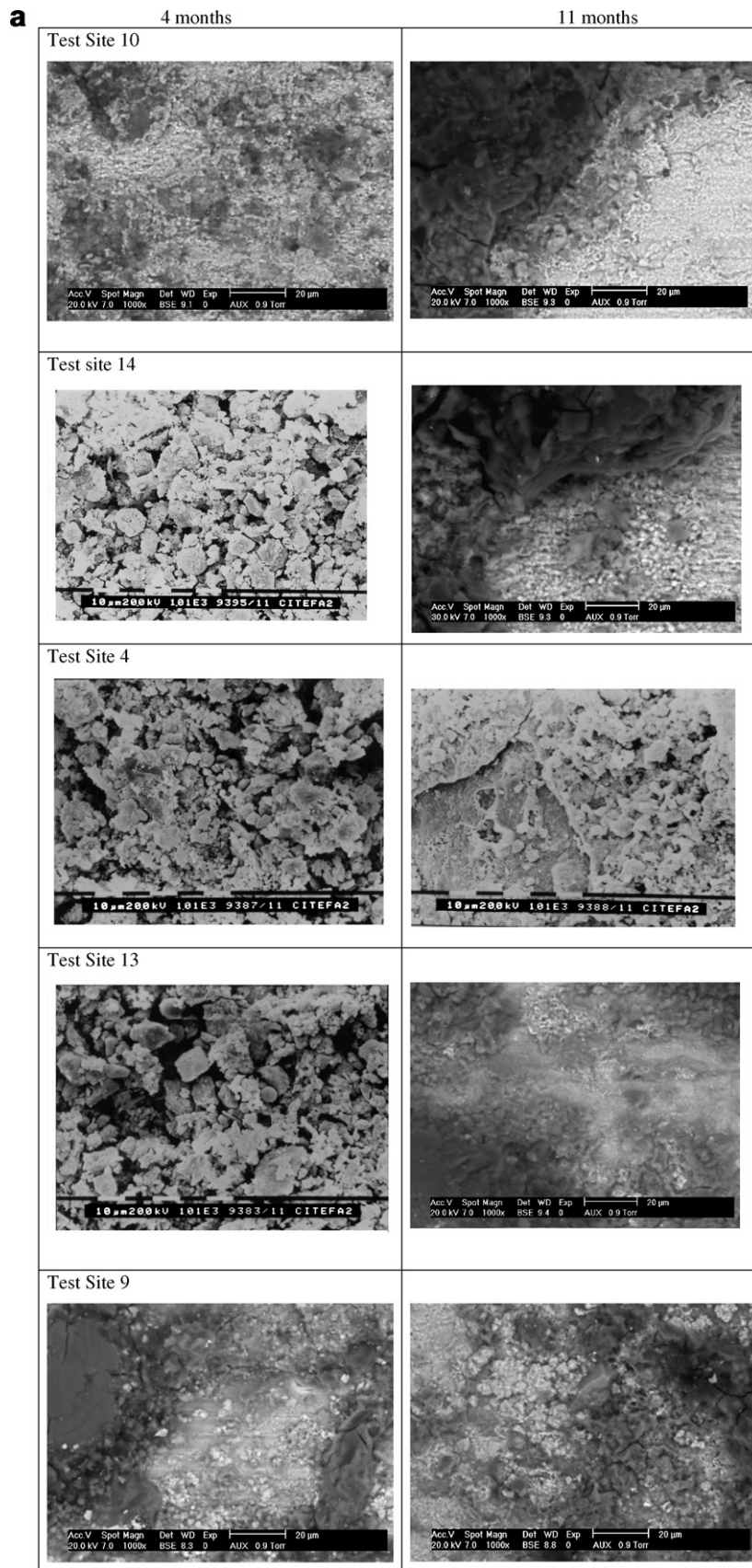
Fig. 3. SEM–EDX of copper samples in plan after 4 and 11 month exposure in all the test sites. (a) SEM aspect. (b) EDX on the corrosion products.

b	**4 months**	**WT (% W/W)**					
	ELEMENT	**S10**	**S14**	**S4**	**S13**	**S9**	**S5**
	Na	21.09	3.72	6.49	6.49	8.45	10.42
	Mg	2.03	2.56	3.39	3.39	---	---
	Al	7.13	19.9	21.01	21.01	6.36	10.62
	Si	7.75	37.78	19.12	19.12	12.74	5.40
	S	7.21	10.89	8.63	8.63	19.01	14.38
	Cl	4.39	0.45	0.54	0.54	1.26	4.09
	K	0.89	2.35	1.33	1.33	0.43	0.61
	Ca	3.06	6.59	5.85	5.85	8.43	3.01
	Fe	1.40	8.97	7.82	7.82	12.35	4.84
	Cu	43.64	6.05	24.61	24.61	27.83	37.65
	Zn	1.35	0.67	1.27	1.27	3.16	8.97
	11 months	**WT (% W/W)**					
	ELEMENT	**S10**	**S14**	**S4**	**S13**	**S9**	**S5**
	Na	4.40	2.78	---	3.79	4.02	2.85
	Mg	2.80	4.59	1.27	3.66	2.15	2.65
	Al	21.43	23.33	12.25	17.46	15.38	11.55
	Si	38.68	27.52	15.72	17.19	20.23	18.84
	S	8.90	7.41	2.06	9.54	15.82	17.21
	Cl	0.17	1.13	12.91	1.81	---	1.57
	K	2.27	1.37	0.67	0.45	1.01	1.45
	Ca	7.28	1.40	0.59	1.14	7.81	5.51
	Fe	7.73	8.20	3.83	5.66	8.79	11.77
	Cu	6.35	20.81	49.44	37.99	19.13	23.17
	Zn	---	1.51	1.28	1.33	5.69	3.46

Fig. 3 (*continued*)

pollutant deposition rate but to the dissolved amount controlled by the distance to the sea shore line. The sea shore distance would control both the amount of water, defined as the TOW, and salt through the fog reaching the test samples. Fig. 3a shows the in plan morphology of the samples exposed during 4 and 11 months in test sites 10, 14, 4, 13 and 9. The TOW, really affecting the metal corrosion rate is not the one estimated according to the technique described in the ISO Standard 9224 [18], but can be more precisely revealed by comparative EDX analysis of the samples at both exposure times of Fig. 3b. Weather its "real value" is not measured "in situ" it can be considered proportional to the salt fog attaining the samples. As the amount of Cl^- polluting the atmosphere does not almost affect corrosion as compared to SO_2, for this set of extremely high SO_2 content and almost uniform Cl^-, the Cl% determined through EDX is very useful as a more appropriated tool than the procedure described in ISO 9224 [18] to compare the TOW of the respective sites.

It seems to be more useful in these very highly SO_2 contaminated atmospheres and medium Cl^- pollutant contents to compare the respective Cl% in the EDX on the corrosion products to those collected as deposition rates at the sites. However, from a graph intended of SO_2 or $SO_2 + Cl^-$ in the atmosphere as a function S or S + Cl% results with EDX was evident the effect of rains on certain test samples. As it had been demonstrated by Rajagopalan et al. for steel [22] there is not a direct relationship between pollutant level in the atmosphere and in the corrosion products. However, this effect of rains in washing off the soluble salts temporarily retained in the steel corrosion products, should not significantly affect copper because of the pollutants integration in the insoluble copper corrosion products might not be lost during rains and a good correlation could be expected. A small weight loss caused by the corrosion products formed plus copper runoff but, even when the latter contribution is quite low in the first steps of patina formation, some decrease from the products film could be determined during rains [11].

Then, the weight loss seems also be proportional to the water available to solubilise corrosive contaminants. Thus, lowest similar values for sites 14 and 4 as compared to site 10 could be due to the important distance increase responsible for almost the same total Cl^- from the first to the second and third sites, but proportional to the atmospheric Cl^- and consequent TOW and weight loss. The higher distance from site 4 than 14 from the sea shore can be appreciated in a lower weight loss for site 4 that can also be attributed at a smaller TOW proportional to the distance difference.

Similar distances to the sea of sites 13, 9 and 5 the inverse order in Cl^- deposition rates would suggest a parallel efficiency order in TOW loss, justifying the relative low effect on weight losses at all those places for analogous Cl^- (and TOW) but so higher and different atmospheric SO_2 contents more according to 11 than to 4 months exposure and to EDX S%.

4.2. Morphology and chemical analyses

The interest in analysing copper atmospheric corrosion is based on its corrosion products characteristics, especially
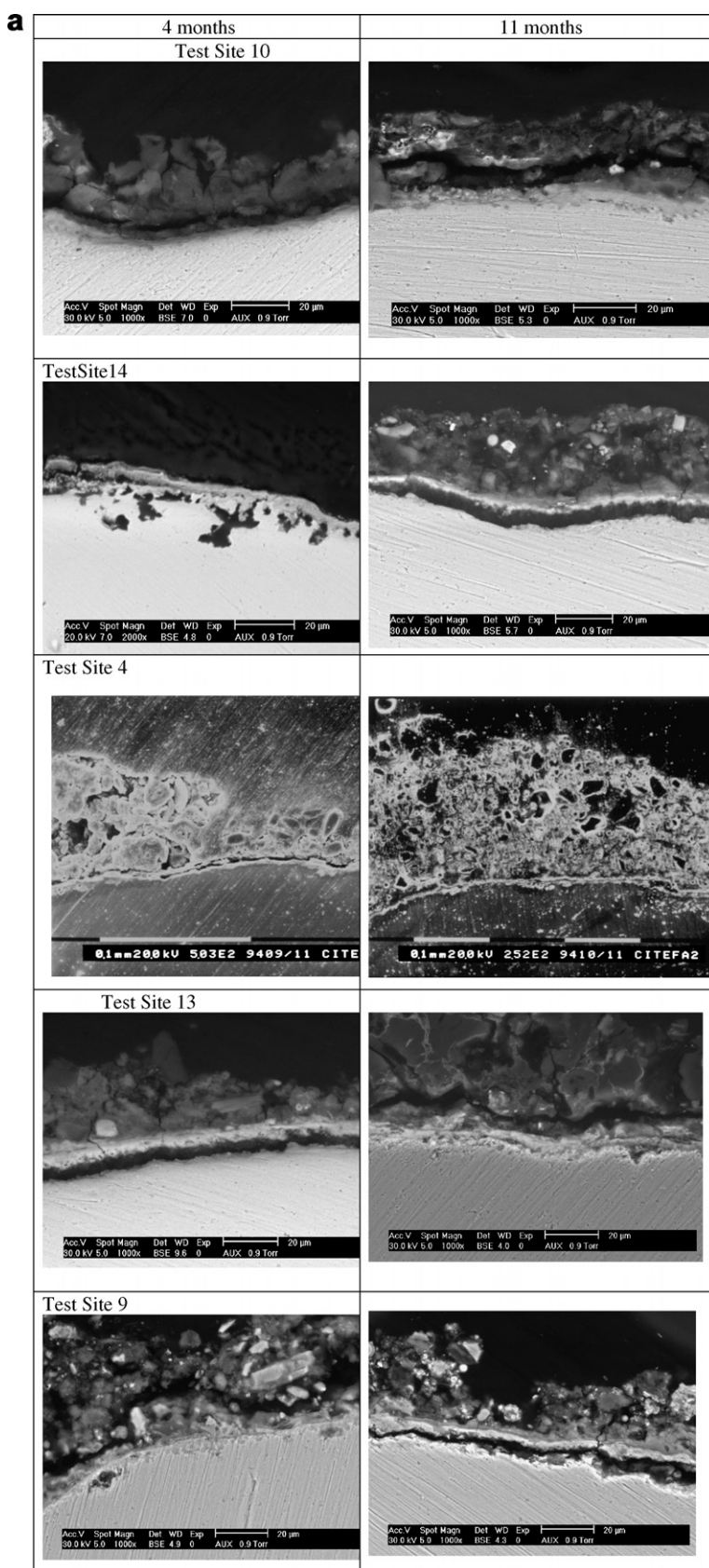
Fig. 4. Transverse cross section of copper samples after 4 and 11 months in all the test sites. (a) SEM/ESEM aspect in tests sites 10, 14, 4, 13 and 9. (b) ESEM–EDX aspects of a sample after 11 months exposure to the highest SO_2 in site 5. (c) ESEM–EDX of a longitudinal polished cross section after 4 months exposure in site 4.
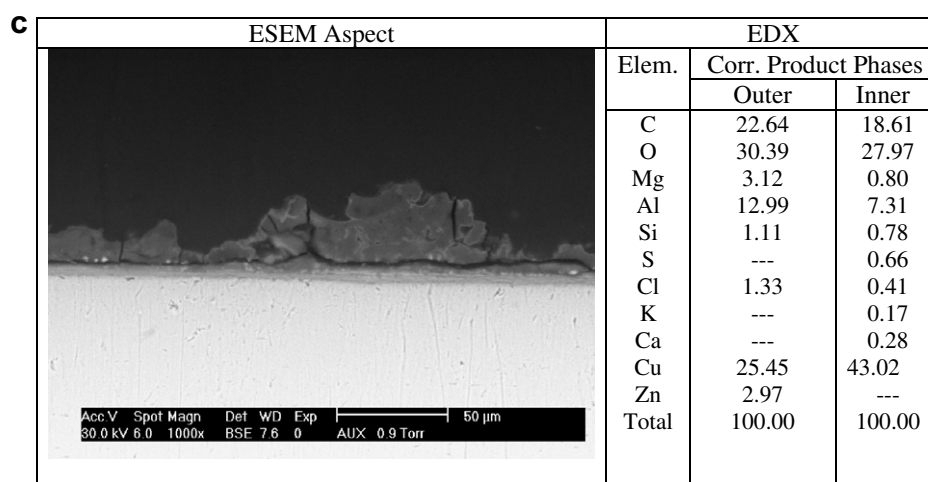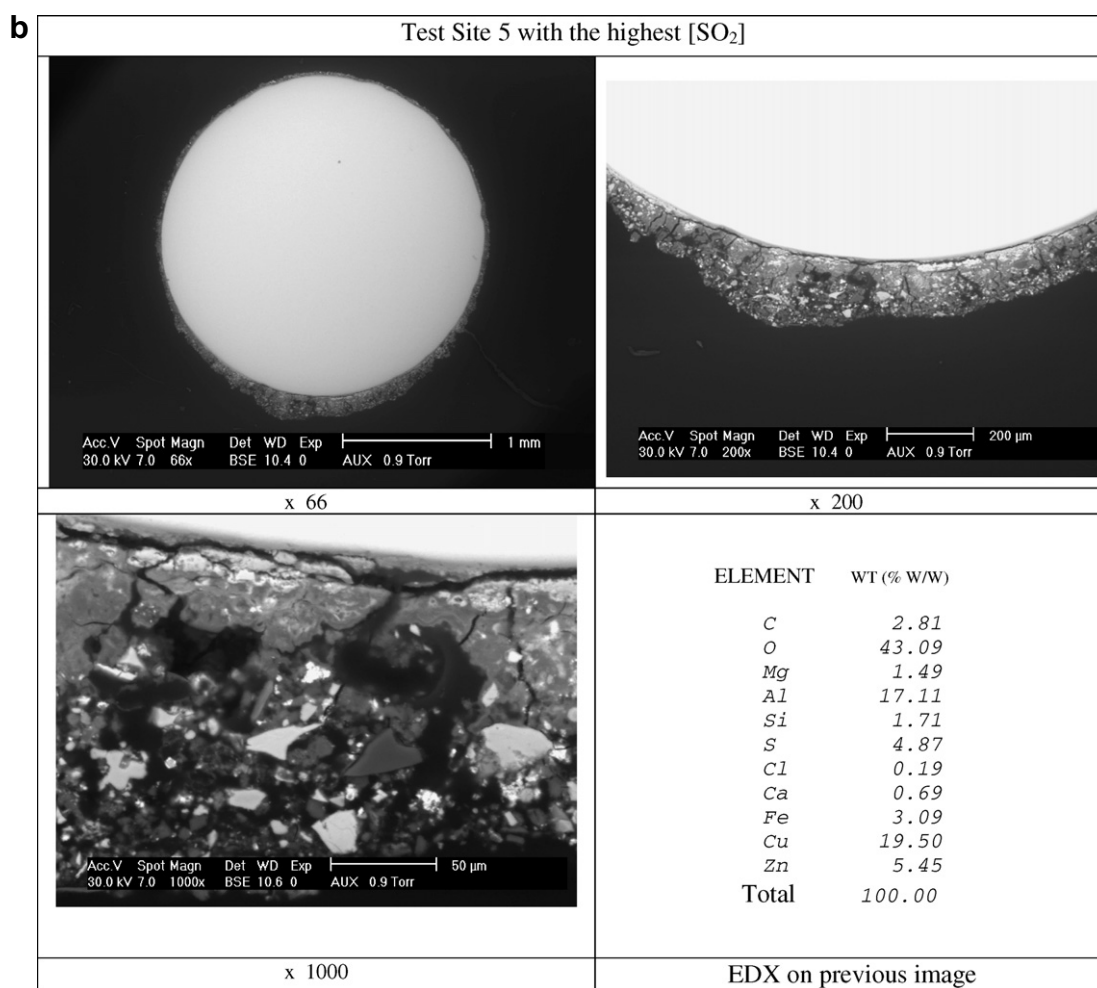
b

| Test Site 5 with the highest [SO₂] |

x 66   x 200

ELEMENT	WT (% W/W)
C	2.81
O	43.09
Mg	1.49
Al	17.11
Si	1.71
S	4.87
Cl	0.19
Ca	0.69
Fe	3.09
Cu	19.50
Zn	5.45
Total	100.00

x 1000   EDX on previous image

c

ESEM Aspect	EDX	
	Elem.	Corr. Product Phases
		Outer	Inner

Elem.	Outer	Inner
C	22.64	18.61
O	30.39	27.97
Mg	3.12	0.80
Al	12.99	7.31
Si	1.11	0.78
S	---	0.66
Cl	1.33	0.41
K	---	0.17
Ca	---	0.28
Cu	25.45	43.02
Zn	2.97	---
Total	100.00	100.00

Fig. 4 (*continued*)

its very low solubility in rain water. This appears as the responsible factor promoting patina formation but also because most of its corrosion products include the environmental pollutants. This unique characteristic as compared to most cooperatively studied metals Fe, Zn and Al, submitted to great variety of atmospheric conditions [9,13,15] allows copper samples to reveal pollutant contamination at exposure sites even when their detection in the corrosion product films were not proportional to the atmospheric content [22,23,14,3].

The wet–dry–wet deposition cycles during atmospheric corrosion generally involve solid elements not considered,
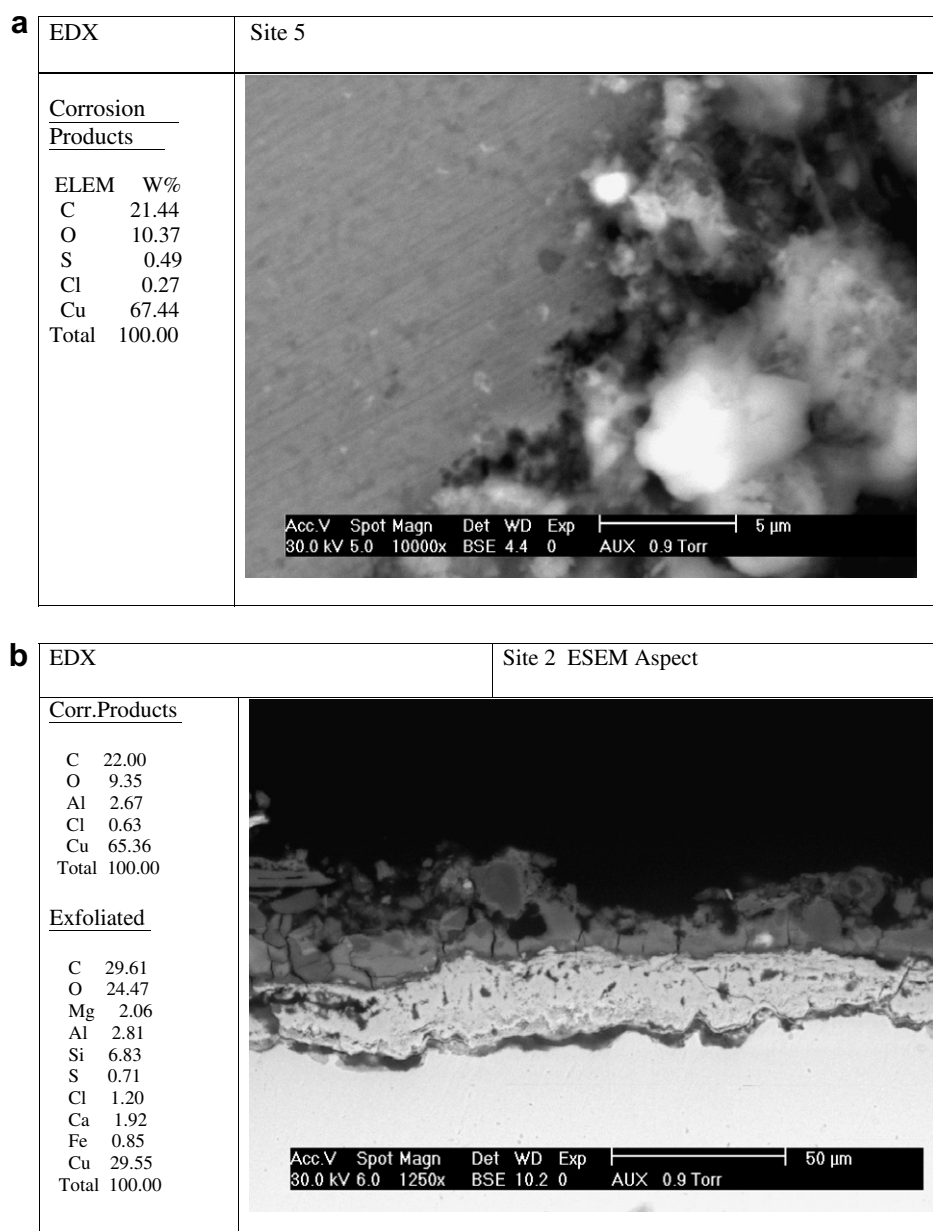
a

EDX	Site 5
Corrosion Products ELEM W% C 21.44 O 10.37 S 0.49 Cl 0.27 Cu 67.44 Total 100.00	

b

EDX	Site 2 ESEM Aspect
Corr.Products C 22.00 O 9.35 Al 2.67 Cl 0.63 Cu 65.36 Total 100.00 Exfoliated C 29.61 O 24.47 Mg 2.06 Al 2.81 Si 6.83 S 0.71 Cl 1.20 Ca 1.92 Fe 0.85 Cu 29.55 Total 100.00	

Fig. 5. ESEM–EDX cross sections comparison of pickled samples after 11 months exposure (a) in the marine-industrial site 5 (b) in the heaviest Cl⁻, site 2 [3].

as soil coming from the ground, amongst the corrosiveness classification in ISO standard 9224 [18]. These not always inert elements contribute according to their properties to increase or delay the weathering process rate. They influence, however, the time spent in attaining the main traditional patina characteristic its "green colour". The worldly increasing atmospheric pollution in last decades was considered a decisive factor for a faster patina formation, even evaluated through this subjective parameter [6].

A more scientific proposal for patina definition [10], than its colour involves the electrochemical current density measurement in determined conditions, or its reciprocal the corrosion products film protectiveness, in quantitatively defined environments [24–26,14,3].

4.2.1. In plan analyses

The generalised concept of the uniform penetration of atmospheric corrosion is once again demonstrated to be a limited characteristic by the magnification applied to observation. The morphology analysis always shows localised attacks associated to metal heterogeneities or to uneven atmospheric pollutants deposition (soil, water condensation, heterogeneous rain distribution according to the structure design, sheltered zones, etc.).

The uneven metallic attack is generally masked by the corrosion products film. But when polished cross sections are observed, crest to valley height increase for corroded surface with the atmospheric pollutant content and exposure time are revealed, as well as the corrosion products
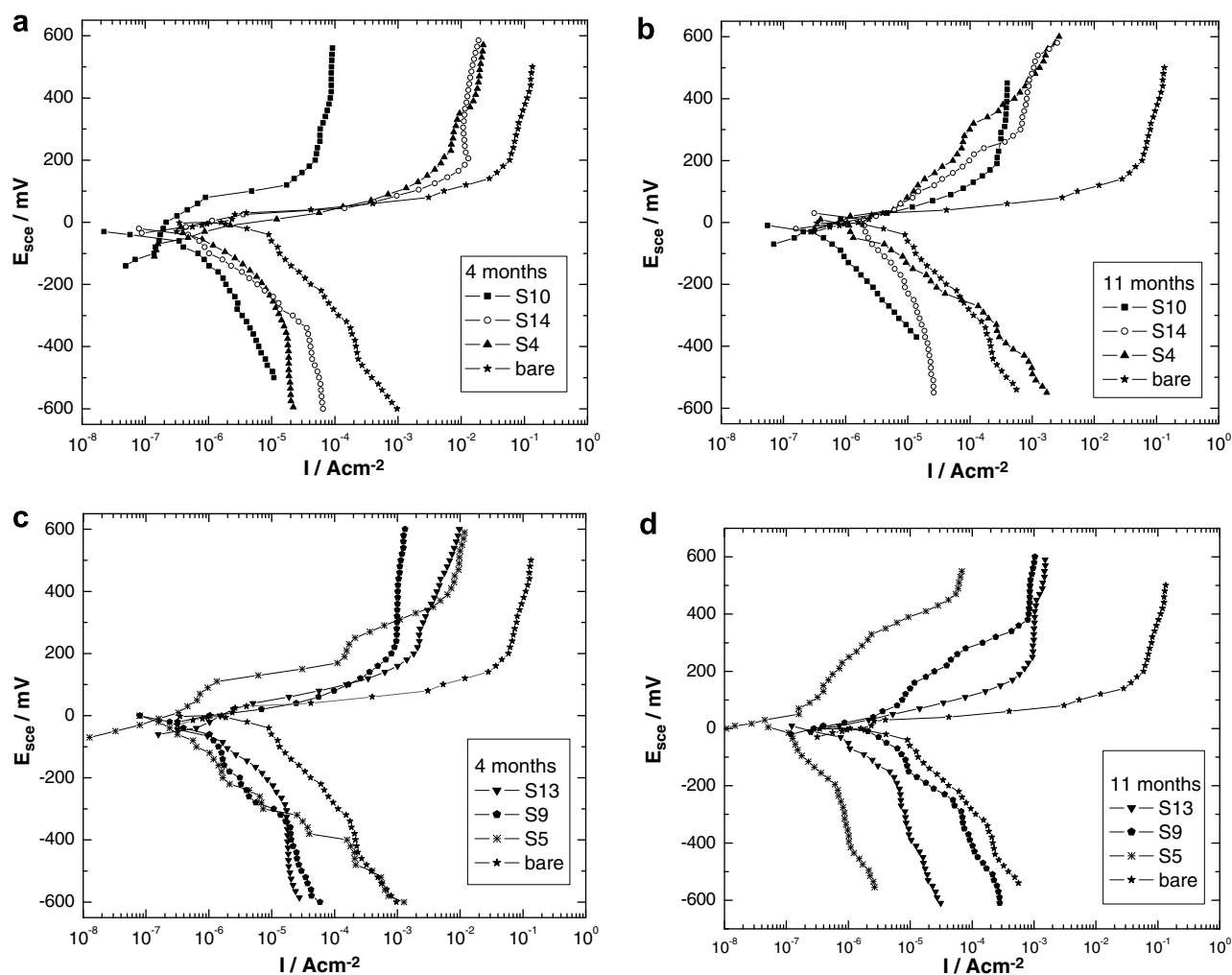
Fig. 6. Polarisation of copper after exposition in the 6 marine-industrial sites as compared to non-exposed bare Cu, anodic in the absence of oxygen and cathodic in air saturated 0.1 M Na₂SO₄ solution after 4 and 11 months. (a and b) Test sites 10, 14, 4 and bare Cu. (c and d) Test sites 13, 9, 5 and bare Cu.
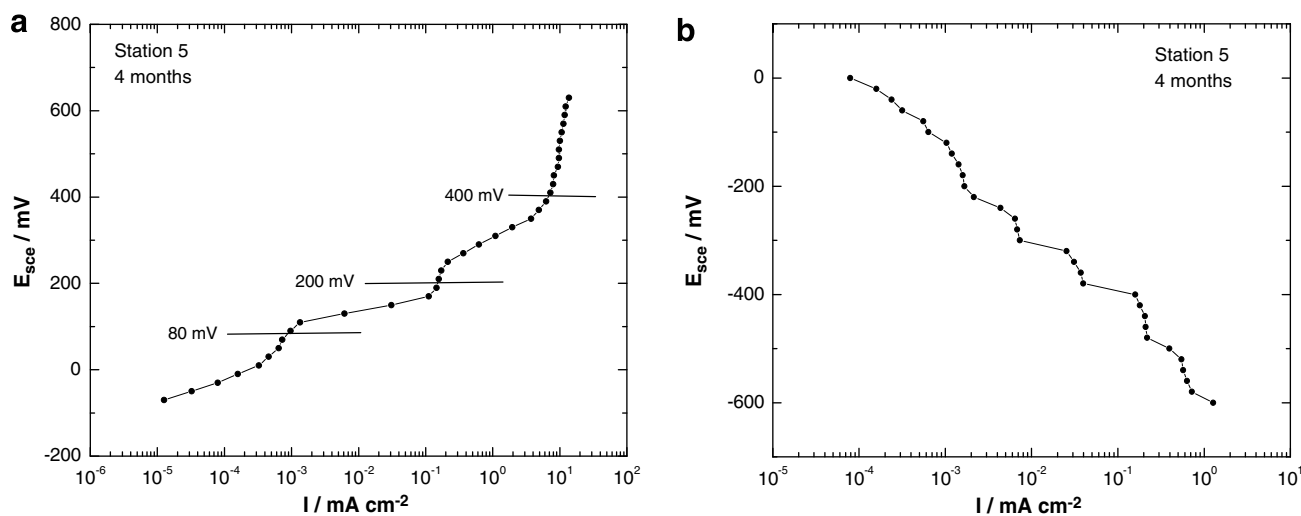

Fig. 7. Polarisation of copper in 0.1 M Na2SO4 solution after exposition in the marine-industrial site 5. (a) Anodic in the absence of air. (b) Cathodic in air saturated solution. (c) ESEM aspect of the corrosion products formed at the 3 different plateaux of (a). (d) EDX on the corrosion products at the 3 plateaux of (a).
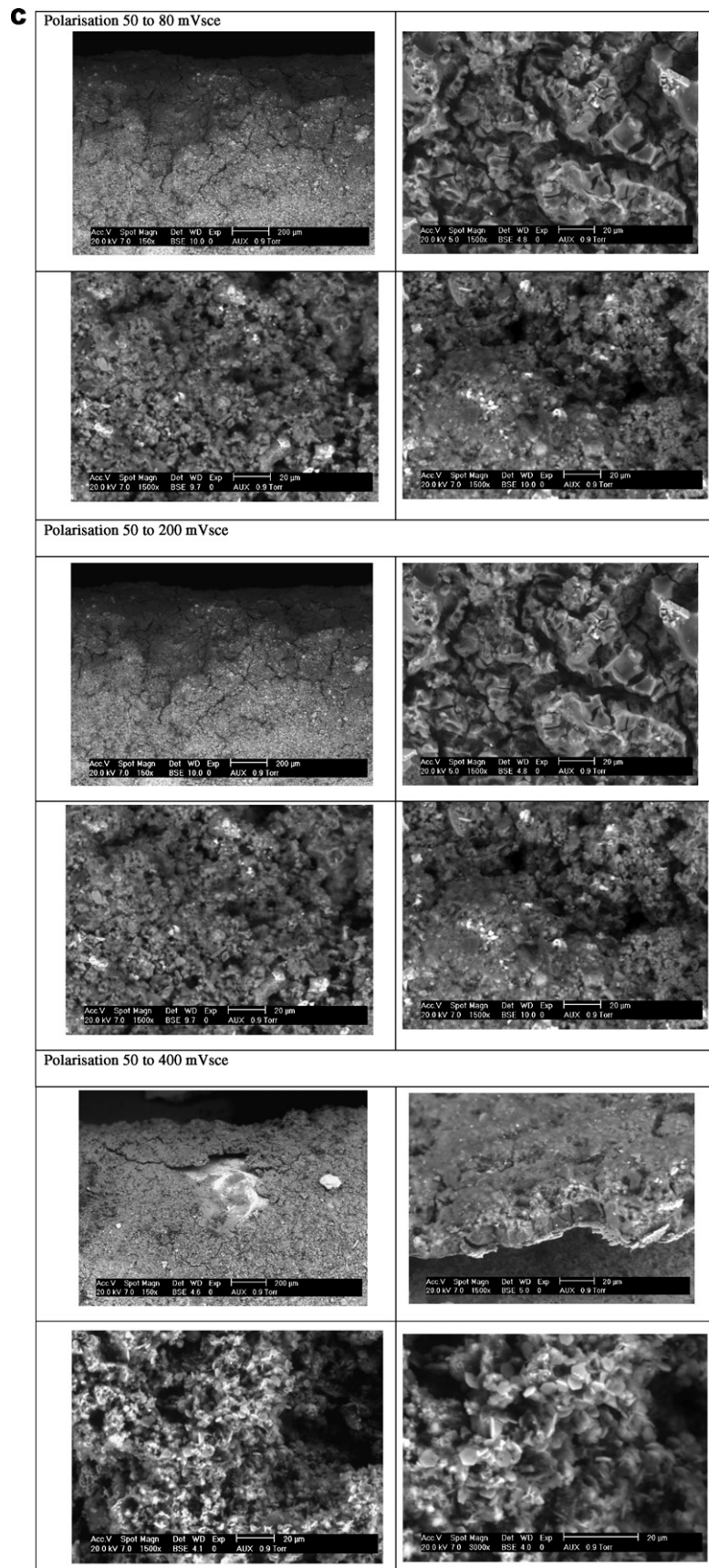
Fig. 7 (*continued*)

d

Element / Potential	WT (% W/W)		
	50-80 mVsce	50-200 mVsce	50-200 mVsce
C	0.50	2.81	7.66
O	24.21	43.09	23.00
Mg	1.59	1.49	2.50
Al	7.01	17.11	6.63
Si	2.28	1.71	2.75
S	4.88	4.87	1.67
Cl	0.85	0.19	1.44
Ca	3.78	0.69	0.92
Fe	6.96	3.09	1.03
Cu	18.52	14.07	42.71
Zn	15.32	5.45	9.69
Pb	14.11	5.43	-----
TOTAL	100.00	100.00	100.00

Fig. 7 (*continued*)
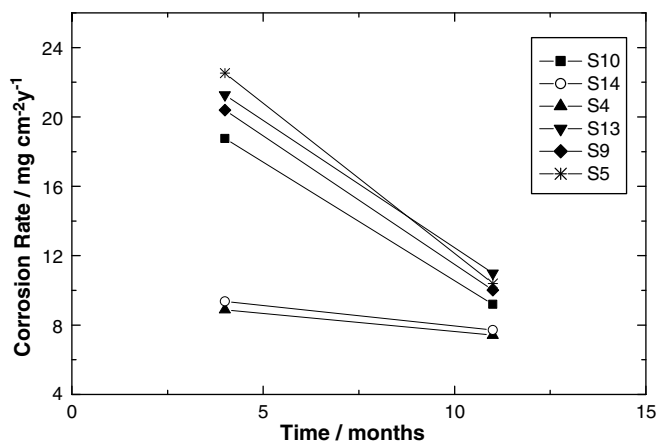
Fig. 8. Slope of graph in Fig. 2 as a function of copper exposure time in the 6 marine-industrial atmospheres after 4 and 11 months exposure.

film thickness, especially for the longest exposure period and the lowest magnification (Fig. 4b). In plan views of surfaces after corrosion products elimination by acid pickling also reveal this uneven penetration morphology.

4.2.2. Transverse and longitudinal cross section analyses

In Fig. 4a the SEM/ESEM aspect in polished transverse cross section after both exposure periods at test sites 10, 14, 4, 13 and 9 show evidence of the relative corrosion rates through the corrosion product film thickness and compact-

ness enhancement with the industrial pollutant content and time increase. Details of the inner and outer corrosion products faces show the higher spurious elements deposition coming from the soil, which contribute to the outer film compactness with its consequent protectiveness increase.

The main details for the highest SO_2 concentration at site 5 can be seen for the lowest magnification in Fig 4b. Complete view of the transverse cross section (at around $70\times$), demonstrates the irregular corrosion products film thickness around the circumference, associated to uneven TOWs, as well as in all high polluted test sites in different materials wires [14,3]. On the contrary, low contaminated atmospheres show a more regular corrosion products growth through thinner and more uniform corrosion product films [14,3].

Their interface with the under laying metal was always less intensely attacked with copper pitting evidence but neither intergranular attack nor propagation. Smaller particles developed at a more uniform corrosion rate producing a smoother outer surface.

At 200 magnification the corrosion products film vision is limited to a sector of the circumference, but a more detailed aspect of the interface allows to estimate the damage intensity on the metal, particle sizes diminution of the products favouring compactness, soil pollutants incorporation, etc.

At 1000 magnification very clear comparisons can be done amongst the atmospheric aggressiveness, the type of
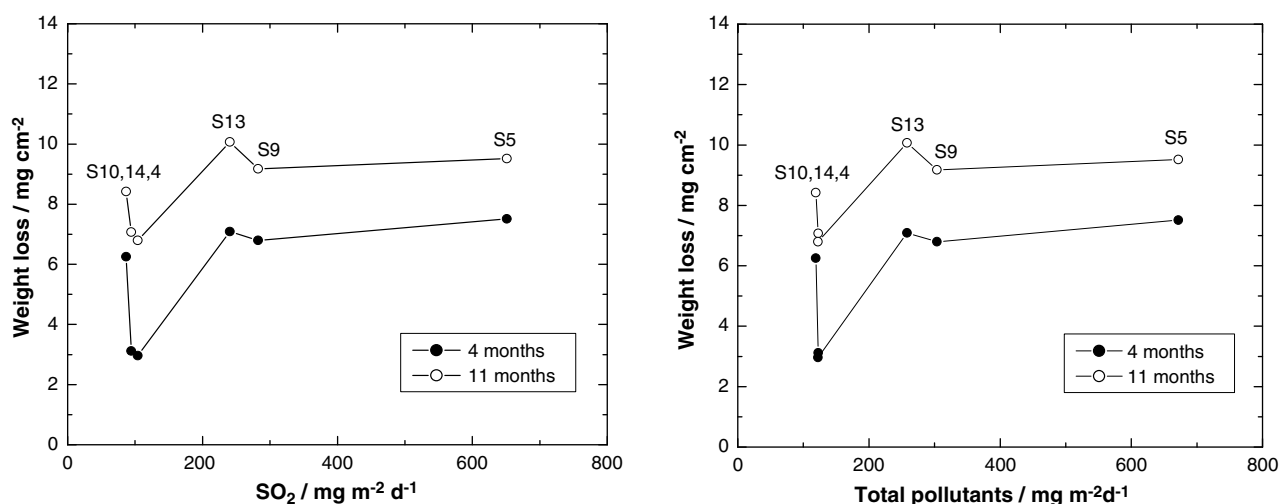
Fig. 9. Weight loss of copper in the 6 marine-industrial stations for the two exposure times as a function of (a) the SO_2 and (b) the total pollutant contents.
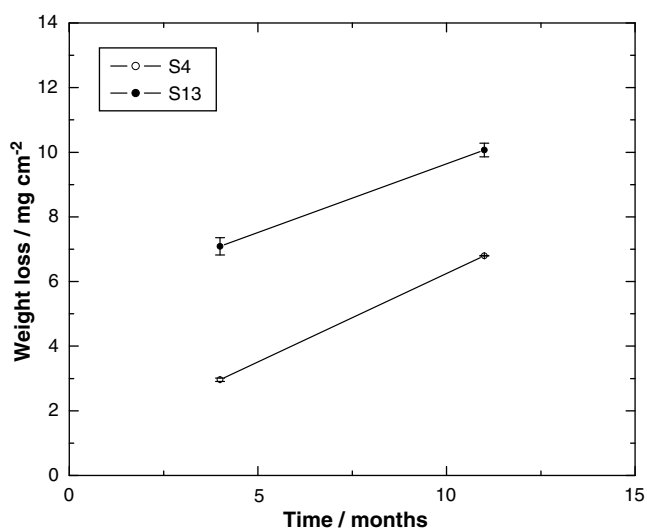

Fig. 10. Maximum and minimum weight loss deviation of copper in the 6 marine-industrial stations 4 and 13.

metal attack susceptibility and the corrosion products thickness, but at 2000 magnification, the deepest pitting attack corresponded to site 14 and at 1000× to site 10 for highest Cl^- and lowest SO_2. This may be related to their highest relative Cl^- detrimental effect on copper and the SO_2 protective effect. In none of them intergranular attack was found.

The longitudinal cross section shown in Fig. 4c also revealed the absence of attack in spite of the extrusion mechanical effect, which could have been attributed to the highest atmospheric SO_2 protective affect against this form of copper attack. The cross sections of samples retired from sites 13 and 9, for the lowest Cl^- and very high SO_2, showed copper soft pitting but it did not propagate through any intergranular attack.

Cu samples in polished cross section after each exposure period showed in these test sites two layered structure, as it

had been previously found for steel [24], Zn and Al [25] and Cu [26] in other atmospheres.

According to EDX results on each SEM/ESEM micrograph of corrosion product layers from Fig. 4 abundant soil contaminants are always involved for each site and exposure period through the wires film thickness. Always insoluble in rain water copper corrosion product compounds are formed as basic chloride (only at site 10) or sulphates (except for sites 14 and 4, only after the first 4 months exposure). During the TOW of the wet–dry–wet cycles they also incorporate soil solid pollutants in an outer contamination layer, as it was generally found other authors during outdoor corrosion tests [9,28–30].

Longitudinal cross section from the test site 4 was also shown in Fig. 4c, corresponding to the lowest weight loss values. That enabled us to determine the attack nucleation morphology and its connection with the ambient pollutants on the expectedly retained lamellar structure left behind by the wire extrusion process. However, there was not attack nucleation that could have been associated to this hypothesis which in this highly aggressive atmosphere could have been masked by abundant exfoliating attack. This aspect had previously been appreciated on pure Al and on its AA 6201 alloy in these atmospheres, but their metallographic aspect were not reported because the transverse cross sections should obviously have shown this wire attack [14].

This behaviour was even not found in samples exposed at site 10 in spite of being the atmosphere with the maximum Cl^- and TOW for the minimum SO_2 of the set.

The ESEM aspect of a pickled sample after 11 months exposure at site 5, shown in Fig. 5a, as well as in 7d of a previous paper of this series [3], evidenced a much less deep attack penetration on Cu as compared to Al and its AA 6201 alloy [14] in the heaviest SO_2 polluted atmosphere of this study. Same aspect in the heaviest Cl^- polluted site 2 is shown in Fig. 5b to compare present findings with other attack mechanisms, especially since their nucleation,

respect to highly polluted marine atmospheres and to other base metals.

Comparison of Fig. 5a and b contrary to the expected, with samples retired from the highest Cl^- polluted site 2 to the one with the highest SO_2, the latter did not show exfoliation, even observed at 10,000 magnifications. The EDX Cl% differences amongst the corrosion products in both atmospheres seems too small to justify the exfoliated film found after exposure to site 2, through intergranular attack in the presence of Cl^- and slightly lower S.

The susceptibility of copper to nucleate and propagate exfoliating attack through grain boundaries observed in high Cl^- atmospheres in a previous paper [3], especially in the highest Cl^- contaminated site 2 is shown in Fig. 5b, while it did not occurred even in the presence of highest atmospheric SO_2 pollutant (Figs. 4 and 5).

This would evidence an intense SO_2 protective effect against intergranular attack in spite of the moderate Cl^- always present and a of the broad concentration spectrum tested for the main industrial pollutant.

4.3. Solid pollutants

During atmospheric corrosion it is very frequent to observe solid pollutants particles incorporated from the soil. Wet corrosion products along the whole exposure time can be appreciated through SEM/ESEM–EDX in plan as in cross section analyses from the metal to the outer film surface. The presence of high Si and Al, as well as different proportions of Ca, Mg, Fe, Na, Zn spurious elements through the whole test sites corrosion product surfaces can be appreciated in the EDX of Figs. 3b and 4a–c after both exposure periods. The relative airborne amount does not follow any regular pattern with time, mainly dependent of the wind regime, turbulence and predominance, controlled by the transport to the sample surfaces, generally less considered as compared to gaseous and marine aerosol pollutants.

Also in urban areas where the SO_2 control decreased the incidence of this important contaminant the relative relevance of other corrosive gases as NO_x and O_3, a well as soiling effects, are being considered. The great importance of atmospheric chemistry involved many species studies lately in connection with the global change, air quality and corrosion [11].

During the first 4 months the maximum (Si + Al) were found (Fig. 3b) in samples from site 14 (58%) while after 11 months the most soil contaminated site was 10 (60%). In this site also high C% was determined through ESEM-EDX, also revealed in the X-ray diagrams. The presence of high EDX values for Si was generally accompanied by strong quartz lines involved in the respective corrosion products X-ray diffraction characterisation (Table 2). High EDX values for Na, in sites 10 (21%) and 5 (10%) after the first exposure period however, did not always fit the presence of NaCl found through X-ray. Also Cl was found in low% in EDX, except in sites 10 and 5 after 4 months

and site 4 after 11 months, while NaCl was found through X-ray diffraction as a major component (M) in sites 14, 4, 13 and 5 after the first 4 months period and in sites 14, 4 and 5 after 11 months exposure. The remaining crystalline substances identified were only copper corrosion products, as patinas components due to their low solubility in rain water (Table 2).

Many apparently inert elements can be seen in the EDX on micrographs, acting as crack and void filler throughout the corrosion product layers. But, according to their aggressiveness and solubility characteristics, some of them may improve compactness cooperating to the film protectiveness, or on the contrary, being water soluble or hygroscopic, others are prone to increase the TOW [9], promoting corrosion nucleation and propagation. They can also solubilise salts accumulated in Cl^- and/or SO_2 polluted atmospheres, increasing their relative type and magnitude of incidence as part of the corrosive electrolytes inside the film.

4.4. Anomalous weight losses

The copper weight loss as a function of time shown in Fig. 2 does not allow analysing the partial effect of the atmospheric pollutant proportions because of the much higher SO_2 as compared to Cl^-. However, the ESEM aspect of pickled cross sections of samples exposed to the highest Cl^- [3] and SO_2 show that the weight loss must involve loose grain detachment on the entire wire surface in marine environments but not in these atmospheres.

The interesting protectiveness characteristics achieved in previous studies [24–26] for the corrosion products formed in marine environments apparently do not seem to occur in these industrial aggressive atmospheres. However, the evidenced slow weight losses increase with time, shown in Fig. 2 reveals the same protectiveness trend, especially in the heaviest SO_2 polluted test site 5, as can be seen in Fig. 8.

Remains of the pickling process sometimes are not easy to be efficiently eliminated or it takes many immersions in the cleaning solution according to the aggressiveness of the atmosphere. It is more frequent to have remains left when the samples had been exposed to atmospheric conditions producing very adherent corrosion products respect to other sites simultaneously tested. This generally happens after marine than industrial exposures. Increase in time needed for the complete removal respect to prescribed [21] can give a measure of the corrosion products protectiveness on the metal. Comparing the two images of Fig. 5a and b it is evident that the picking efficiency was lower in site 2 (related to the Cl^- presence in contact with the metal and penetrating through grain boundaries) than in site 5, where much less corrosion products remained and no intergranular attack can be appreciated.

From EDX results in Fig. 3b it can be seen that the pollutants found in the corrosion product surface are no correlative of their deposition rates at the test site. In the case

of copper, even when the products formed mostly involve the atmospheric pollutants there is not a direct relationship among both types of determinations.

The amount of liquid water necessary to dissolve the very high SO_2 pollutant content seems not to be enough for its quantitative participation as electrolyte in the film. Even when the TOW was determined from the ambient parameters T and RH, these are neither certainly "real" values on all sites nor metals. Water condensation mostly depends from both parameters relative changes than form their absolute values. The meteorological data shown in Fig. 1a–d are common for all the Region, but the TOW or liquid water available vary from one to other test site and also from sample to sample, according to the hygroscopic properties of the corrosion products and particulate material covering the metal surfaces. Thus, they influence the corrosion products protectiveness.

This behaviour, that had been observed for Al and its alloy 6201 in the marine test sites of this set, as shown in Fig. 9a–d [14], and for Cu in the most aggressive marine atmospheres (Fig. 9b [3]) was also found in these industrial test sites.

Not only the mass loss vs time slopes but also from polarisation in 0.1 M Na_2SO_4 electrolyte the protectiveness increase with SO_2 has been demonstrated, as can be seen from Figs. 6c–d and 8.

4.5. Protectiveness of corrosion products

As it was discussed in the previous paper of this series [3] the corrosion products of a metal are responsible for its corrosion rate decrease with time. Opposite effects could be observed for different metals in a same environment depending on the characteristics of the products they form. The most evident results were demonstrated through their weight loss as a function of time. The relative values and the slopes vs time of those data are the most significant figures for this analysis. Copper samples behaviour in the test sites we are comparing can be derived from Fig. 2 and from their slopes in Fig. 8. Both of them showed interesting differences to focus the discussion providing enough data to justify their relative values to disclose the comparative causes.

The lowest lines in Figs. 2 and 8, corresponding to sites 4 and 14, show the less protective products for the minimum corrosion rate vs. time. That means that those sites have the less aggressive atmospheres to copper (Fig. 2) and also that there is a very slight protectiveness decrease with time (Fig. 8). This is in good agreement with their maximum distances from the sea and from the SO_2 pollutant source. However, they do not have the lowest SO_2 pollutant deposition rates. Site 4 evidences the lowest corrosion rate in spite of having a higher SO_2. The cause for this behaviour must be associated to its lowest TOW, in spite of its minimum barrier effect respect to all the other sites, included site 14, due to its slightly higher altitude (47 vs. 41 mosl), but longest distance to the sea shore.

The next two lines, for sites 10 and 9 show very near but much higher corrosion rates (Fig. 2) according to their relative SO_2 and correlative much higher protectiveness. Site 9 has lower Cl^- than 10, but 3.2 higher SO_2, for a higher barrier effect and slightly lower distance to the sea that could increase its TOW respect to site10.

For sites 13 and 5, the latter shows a lower corrosion rate and consequently higher protectiveness, for its 2.7 higher SO_2 and similar Cl^- contents.

Another way to assess the film protectiveness on the metal is through the electrochemical polarisation behaviour. Anodic as well as cathodic curves shown in Fig. 6a reveal increasing polarising effect due to the corrosion products formed during 4 months for sites with increasing SO_2. This result can be explained by comparison with EDX from Fig. 3b which highest Cu% can be associated to the protectiveness of their products shown in Table 2. Lower intermediate anodic currents are in good agreement with SO_2 while cathodic ones are less coherent. For 11 months, on the contrary the most protective samples are those coming from sites 4 and 14 in that increasing order for the anodic curves, while the high Si% associated to quartz content decreased the relative protectiveness of the site 10 film, according to EDX data and compound shown in Table 2. Cathodic curves did not evidence such a clear correlation for this second exposure period.

For the other set of test sites, analogous criterion provided the same interpretation for both exposure periods, except for a different shape in anodic and cathodic curves from site 5. Cathodic results for these site are however consistent with the anodic behaviour. The high Cu content revealed in site 13 from EDX for the second period did not produce a correlative higher protectiveness as compared to the site 9 samples, except for the first 100 mV anodic potential.

Samples from site 5, due to their very different anodic as cathodic behaviours, even without changes since 4 up to 11 months exposures, deserve an especial analysis. As compared to the results in the other test sites their corrosion products showed the highest protectiveness on copper from the open circuit potential up to around 400 mVsce, with three electrochemical plateaux at different potential intervals. The increasing current densities with the anodic and cathodic potential scan from the open circuit potential show evidence of partial film dissolution non correlative between both polarisation branches. Morphology and elemental analysis on samples after the anodic curve, allowed verifying through ESEM micrographs and EDX%, shown in Fig. 7, the mentioned increasing differential dissolution approaching the limiting current attained for site 13. The relative low atmospheric Cl^- in these sites do not allow to notice its efficiency increasing copper corrosion in the presence of such unusually high SO_2 atmospheric content.

Once again, the apparently paradoxical results shown for Al, Zn, Cu and steel between Figs. 2 and 8 are also demonstrated in this study for copper in very high SO_2

polluted atmospheres [24–26,14,3]. This not previously found behaviour has been up to now restricted to elevated atmospheric Cl⁻, producing higher protectiveness in most aggressive atmospheres. But this result has now been demonstrated, again for copper, in the presence of these six very high SO_2 pollutant content.

From Fig. 7a and b in the previous paper on pure copper of this series [3], the morphology and elemental film composition in these sites provided a good correlation with the exposed results shown in Fig. 3a and b.

Even for these very high atmospheric SO_2 the best corrosion products protectiveness would provide the longest useful life to the respective copper wire. Unexpectedly, according to Fig. 9 this result corresponded to site 5, the most heavily polluted.

The electrochemical and morphology results demonstrated that the copper corrosion products protectiveness increased as SO_2 concentration increased and the exposure time lengthened. A patina thickening and density increase mechanism could be suggested through their porous components structure. This was revealed by the tree plateaux found during the anodic polarisation of samples weathered at the heaviest polluted site 5.

4.6. Electrochemical analysis

From Fig. 6 the anodic and cathodic polarising effect of the increasing copper corrosion products protectiveness can be appreciated for increasing SO_2 in the test site atmosphere.

As it was previously shown [3] the structure through ESEM provided comparative aspect that could give evidence of the respective protectiveness. For samples exposed at the different test sites more protective films were characterised by higher E_c and lower i_c than those for the witness bare sample in all test sites.

The most interesting case observed in polarisation results was for samples exposed at site 5, as shown in Fig. 7a and b. The morphology of the surface at the three potential plateaux provided the necessary structural evidence to explain the increasing protectiveness with SO_2 for the different polarisation curves. In Fig. 7c polarisation of the corrosion products for increasing potentials demonstrated that the protectiveness of the film decreased for a thinner, less compact and more fractured film structure.

4.7. Evaluation of TOW effect

The not frequent atmospheric contaminant cause combinations, due to variable distances to an industrial plant, and to the sea line, height over sea level (osl) and barrier effects to salt fog different non measured TOW at the test sites should be considered during the results analysis. As the meteorological parameters are common to the Region the T and RH values would produce the same apparent TOW according to the Standard

ISO 9224 [18], giving the same value on all the test sites. However, the results discussion will allow us demonstrating that each test site and metallic surface promotes very different TOWs.

Even when exposed as open helix wires did not evidence the clear difference between sky and ground-ward surface of flat samples, all possible orientations and inclinations, were supposed to produce more even effect of pollutant deposition, washing-out by rains, sun drying, and evaporation of dew by winds. However, transversal cross sections evidenced the uneven thickness of the corrosion products formed all around the wire circumference (Fig. 4b for site 5).

Higher magnification provided detailed information not only of the film morphology compactness, homogeneity, corrosion propagation mechanism and pollutants content, but it also gave idea of its protectiveness mechanism. Properties as adherence and compactness are controlled by Cu compounds and solid pollutants coming from the soil may contribute or be opposite to them.

Once again this work allows verifying that the TOW exclusively estimated as the result of environmental conditions for water condensation, according to ISO 9224 standard [18], is responsible for great errors. In previous studies in five test sites in Argentina that errors were estimated in up to a 400% yearly error [27] for an Antarctic test site. Each metal sample on which water deposition occurs has its own TOW determined by its colour, roughness, hygroscopic character of its surface compounds, orientation, inclination, sheltering from rain and sun, etc. During corrosion propagation surface properties modified their capacity for liquid water retention and further localised reactions increased TOWs scattering on the entire wire surface.

The low real TOW of the Region [24,14,3] and too high SO_2 pollutant in these test sites resulted in liquid solvent limitation to fully dissolve the available contaminants. The similar correlation obtained for weight loss vs. SO_2 and vs. total pollutant levels, not only for each period but also over the whole exposure time, for the much lower Cl⁻ does not allow to propose a mechanism for their relative effect.

However, from Figs. 4 and 5 it is clear that a given interaction between both pollutants occur at grain boundary levels being the extreme cases for sites 5 (immunity) and 2 (exfoliation). The relationship amongst their dissolved relative concentrations determines different type and magnitude of the samples' attack according to both pollutants competition in the respective test site. From site 10, with the highest Cl⁻ and lowest SO_2 the maximum exfoliation could be expected in this atmosphere for a factor around 3 between the protective and the aggressive pollutants. For other rates, the next test site is 14 with similar order of passivating/aggressive ratio, then 4, and so on. From the ESEM aspects in shown in Fig. 4 it can be suggested a competitive mechanism fitting as quantitatively as possible to the described.

4.8. Analyses of the effect of Cl⁻ and SO₂ pollutant contents and other atmospheric parameters

In previous papers in the same test sites for the project involving this study [14,3], the analysis of the corrosive effect of joint pollutants on metal weight loss was represented as a function of the total concentration after each exposure period, as it was also done for copper in Fig. 9a and b. Due to the much lower Cl^- than SO_2 the mass loss as a function of total pollutants was very similar to that as a function of the SO_2.

The analysis of the graph trends, show

1. Results in Fig. 9a and b are in good agreement with those already discussed in Section 4.5, for weight loss as a function of SO_2 as well as total pollutant contents, for sites 14 and 4, respect the sites 10, 13 and 9 according to their Cl^- and distance to the sea shore. However, for almost the same weight losses low TOWs decrease the much higher SO_2 effect at sites 13 and 9, evidencing the liquid water strong effect on them, and especially in sites 14 and 4, as compared to site 10.
2. The height over the sea level increases the long distance marine fog effect avoiding condensation barriers such as trees or buildings. The fog arriving to samples produced parallel Cl^- and water increasing TOWs due to SW–NE predominant winds from the sea. This would increase metal weight loss in site 4 respect to14, but the opposite effect would predominate if the distance to the sea line had a stronger effect on the weight loss. However, after the 11 months period there is much more Cl in site 4 than in 14, providing a direct evidence of simultaneous longer TOW. Its lower corrosion rate than at site 14 suggest a passivating SO_2 effect.

Comparing sites 13 and 9 this latter produced lower weight loss in spite of its higher Cl^- and SO_2, not only in the atmosphere but also in the corrosion products. Lower Cl than SO_2 in both media should also suggest lower TOW in 13 than in 9, decreasing in the latter the SO_2 contribution to the electrolyte.

Site 5 could have produced lower weight loss than 9 due to its slightly longer distance from the sea shore line, for a little smaller blocking effect of fog, higher Cl^- than SO_2 in the atmosphere. However, as well through EDX after 4 than after 11 months exposure at site 5 there is a higher % Cl and thus higher TOW producing a good correlation whether the main pollutant contribution of 2.3 SO_2 higher than at site 9 atmosphere, finally reveals a high protective effect on the corrosion products with this pollutant content than an aggressiveness increase.

The small Cl% in the corrosion products from almost all sites except for sites 10 and 5 after 4 months through EDX evidences the low effect that this pollutant can have in the electrolyte aggressiveness during the TOW.

This analysis in the marine-industrial test sites, does not offer so scattered data as in the marine test sites involved in previous works of this project [14,3]. All sites in this study are more uniformly distributed respect to the sea shore and SO_2 pollution source distances and similar heights over sea level must produce less evident TOW differences.

Also, the much higher SO_2 as compared to the Cl^-, with higher dew condensation as compared to the marine test sites, would limit the aggressiveness scattering previously found in the pollutants effect [14,3]. Unexpectedly, even in spite of the very elevated SO_2, this atmospheres produced so high corrosion products protectiveness on copper as compared to Al and its alloy, that much lower copper weight losses were measured as has also been seen for low and high Cl^-.

Consequently, such low weight losses also determined in the previous paper on pure copper [3], would discarded any synergic or cooperative effect of both pollutants on copper, as it had been suggested on the bases of Al and its alloy results [14].

Opposite, and as it was proposed in a previous work for similar and higher Cl^- than SO_2 in these atmospheres, the most probable interaction with pure copper [3] seems to confirm a competitive effect of the pollutants, during simultaneously tests performed on all metals.

From these comparative results for the different metals, those exposed in Fig. 9a and b evidence that the mutual surface pollutant effect would be strongly dependent on the tested metal.

Fig. 6 shows evidence of a more corrosive action on copper by Cl^- than by SO_2, triggered through the intergranular different susceptibilities of pure copper to both pollutants in the electrolyte. While Cl^- stimulates the underlying metal exfoliation SO_2 seems to form protective corrosion products.

5. Conclusions

The results obtained during this study include a set of new findings to the approach of copper atmospheric corrosion, electrochemical response on the corrosion products protectiveness, concurrent morphology and effect of main type of pollutants on the patina films formation.

1. The increasing corrosive effect with pollutant concentration observed on the higher atmospheric Cl^- than SO_2 of the marine test sites vs. time and pollutant concentration [3] was not observed during this study.
2. At these marine-industrial sites, Cu showed as low corrosion rates for same Cl^- to those in the lowest Cl^- marine sites, in spite of the additional much higher SO_2 contents.
3. The corrosion products increased protectiveness for increasing SO_2 and exposure time.
4. The low corrosion rates referred in previous conclusions can neither be attributed to low Cl^- in these atmospheres nor in the corrosion product films formed. On the contrary, it seemed to have been the unusually high SO_2 pollutant the main responsible for the high product films protectiveness.

5. These results demonstrated the copper capability to form good protectiveness patinas in highly SO_2 polluted atmospheres.
6. Lower life expectancy was determined for copper wires in the high Cl^- marine sites [3] than in these much higher SO_2 polluted atmospheres.

References

[1] M. Forslund, C. Leygraf, J. Electrochem. Soc. 144 (1997) 113–120.
[2] Morcillo, E. Almeida, M. Marrocos, B. Rosales, Corrosion, NACE 57 (11) (2001) 967–980.
[3] R. Vera, D. Delgado, B.M. Rosales, Corros. Sci. 49 (2007) 2329–2350.
[4] K. Nassau, P.K. Gallagher, A.E. Miller, T.E. Graedel, Corros. Sci. 27 (7) (1987) 648–669.
[5] K. Nassau, A.E. Miller, T.E. Graedel, Corros. Sci. 27 (7) (1987) 703–719.
[6] T. Graedel, K. Nassau, J.P. Franey, Corros. Sci. 27 (7) (1987) 639–658.
[7] X. Zhang, W. He, I. Odnevall, J. Pan, C. Leygraf, Corros. Sci. 44 (2002) 2131–2151.
[8] J.A. Calderón, C.E. Arroyave, Corrosion, NACE 61 (2) (2005) 99–110.
[9] M. Morcillo, E. Almeida, B. Rosales, J. Uruchurtu y, M. Marrocos, Corrosion and protection of metals in the atmospheres of Ibero-America, Part 1, CYTED, Madrid, 1998, p. 568.
[10] B.M. Rosales, R. Vera, G. Moriena, Corros. Sci. 41 (1999) 625–651.
[11] C. Leygraf, T.E. Graedel, Atmospheric Corrosion, John Wiley & Sons, Inc., New York, 2000.
[12] L. Volpe, P. Peterson, in: J.D. Sinclair (Ed.), Proceedings of 1st International Symposium on Corrosion of Electronic Materials and Devices, The Electrochemical Society, Pennington, NJ, 1991, pp. 22–39.
[13] J. Tidblad, V. Kucera, A.A. Mikhailov, Report 30, UN/ECE International Cooperative Program on Effects on Materials, Swedish Corrosion Institute, Stockholm, 1998, 49 p.
[14] R. Vera, D. Delgado, B.M. Rosales, Corros. Sci. 48 (2006) 2882–2900.
[15] D. Knotková, K. Barton, P. Holler, in: R. Baboian, S.W. Dean (Eds.), Corrosion Testing and Evaluation, ASTM STP 1000, Philadelphia, 1990, pp. 80–91.
[16] L. Veleva, L. Maldonado, Brit. Corros. J. 33 (1) (1998) 53–57.
[17] ISO 9223, Corrosion of metals and alloys. Classification of corrosivity of atmospheres, ISO, Geneva, 1991.
[18] ISO 9224, Corrosion of metals and alloys. Guiding values for the corrosivity categories of atmospheres, ISO, Geneva, 1991.
[19] ISO 9225, Corrosion of metals and alloys. Corrosivity of atmospheres- Methods of measurement of pollution, ISO, Geneva, 1991.
[20] ISO 9226, Corrosion of metals and alloys. Corrosivity of atmospheres – Methods of determination of corrosion rate of standard specimens for the evaluation of corrosivity, ISO, Geneva, 1991.
[21] ISO 8407, Metal and alloys – Procedures for removal of corrosion products from corrosion test specimens, ISO, Geneva, 1992.
[22] K.S. Rajagopalan, S. Chandrasekanran, M. Sundaram, P.S. Mohan, in: Proc. 5th. Int. Symposium on modelling on environmental effects on electrical and general engineering equipment, Liblice, 1978, pp. 183–193.
[23] I. Ondelval Wallinder, C. Leygraf, Corros. Sci 39 (1997) 2039–2052.
[24] R. Vera, B.M. Rosales, C. Tapia, Corros. Sci. 45 (2003) 321–337.
[25] J.R. Vilche, F.E. Varela, G. Acuña, E. Codaro, B.M. Rosales, A. Fernández, G. Moriena, Corros. Sci. 37 (6) (1995) 941–961.
[26] J.R. Vilche, F.E. Varela, G. Acuña, E. Codaro, B.M. Rosales, A. Fernández, G. Moriena, Corros. Sci. 39 (4) (1997) 655–679.
[27] B.M. Rosales, Maps of Atmospheric Corrosiveness of Argentina, 1st ed., América Editora, Buenos Aires, 1997, pp. 189–192.
[28] J. Richter, H. Kaesche, Werk. Korros. 32 (1981) 174.
[29] G.C. Wood, J.A. Richardson, M.F. Abd Rabbo, L.P. Mapa, W.H. Sutton, in: R.P. Frankental, J.P. Kruger (Eds.), Passivity of Metals, The Electrochemical Society, Princeton, 1978.
[30] T.E. Graedel, J. Electrochem. Soc. 136 (1989) 204.